NUCLEAR THEORY, Vol. 29 (2010)
eds. A. Georgieva, N. Minkov, Heron Press, Sofia

# Non-Yrast Alternating Parity Bands in a Model of Coherent Quadrupole-Octupole Motion

**N. Minkov**[1], **S. Drenska**[1], **W. Scheid**[2]

[1]Institute of Nuclear Research and Nuclear Energy, Bulgarian Academy of Sciences, Tzarigrad Road 72, BG-1784 Sofia, Bulgaria
[2]Institut für Theoretische Physik der Justus-Liebig-Universität, Heinrich-Buff-Ring 16, D–35392 Giessen, Germany

**Abstract.**

A model assuming coherent quadrupole-octupole vibrations and rotations is applied to describe non-yrast energy sequences with alternating parity in even-even rare-earth and actinide nuclei. Within the model scheme the yrast alternating parity band is composed by the members of the ground-state band and the lowest negative-parity levels with odd angular momenta. The non-yrast alternating parity sequences unite the levels of the $\beta$- bands with respective higher negative parity levels. It is shown that the model successfully reproduces the yrast and the first non-yrast alternating parity bands in the rare-earth nuclei $^{150}$Nd, $^{152}$Sm, $^{154}$Sm and $^{156}$Dy, and the actinides $^{232,236}$U. In the nuclei $^{154,156}$Gd and $^{234,238}$U the available second non-yrast sequences are also described.

## 1 Introduction

A typical manifestation of the reflection-asymmetric quadrupole-octupole deformation in the energy spectra of even-even atomic nuclei is the formation of level sequences with alternating parity [1]. Usually the levels with opposite parity are related through enhanced electric E1 and/or E3 transitions. The negative-parity sequence is shifted up with respect to the positive-parity sequence due to a tunneling of the system between the two opposite orientations along the principal symmetry axis. The magnitude of the energy shift corresponds to the softness of the shape with respect to the octupole deformation. The typical alternating parity band is formed by the members of the ground-state band (GSB) and the levels of the lowest negative-parity sequence with odd angular momenta. In the relatively narrow region of the light actinide nuclei Rn, Ra, Th these two sequences merge into a single rotation band called "octupole band". The octupole band develops in the higher angular momenta and indicates the appearance of quite a stiff octupole deformation. Away from the light actinide region both sequences diverge, but still in some heavier actinides, like U and Pu and some rare-earth isotopes like Nd, Sm, Gd and Dy, they remain related by electric transitions, which indicates the presence of a soft octupole mode in the collective motion.

Various theoretical models have been developed over the years to explain and describe the formation of alternating parity (or octupole) bands in the stiff and soft octupole regimes of coupling between the GSB and the lowest negative-parity sequences in different nuclear regions [2]– [12]. Particularly, a collective model assuming coherent quadrupole-octupole vibrations and rotations [10] was applied to the nuclei $^{150}$Nd, $^{152}$Sm, $^{154}$Gd and $^{156}$Dy with the presence of a soft octupole collectivity. Although the GSB and the lowest negative-parity bands in these nuclei were successfully described as members of a yrast alternating parity band together with the attendant E1 and E2 transition probabilities, a question arises about the validity of such a consideration with respect to the higher-energy (non-yrast) part of the spectrum.

The purpose of the present work is to clarify the above question within the model of Coherent Quadrupole-Octupole Motion (CQOM) [10] by examining the possible formation of non-yrast alternating parity structures in addition to the yrast band. For this reason the model scheme is extended by assuming that the excited $\beta$-bands can be connected to higher negative-parity sequences with odd angular momenta. Therefore, it is supposed that the quadrupole-octupole structure develops along the non-yrast regions of the energy spectrum. Such a study not only provides a test of the model in the higher energy parts of the spectra, but also gives an interpretation of a larger number of data which may guide the experimental search of similar level structures in other nuclear regions. As it will be demonstrated below, the systematic analysis of the non-yrast levels with alternating parity may favour different band-coupling schemes in the different nuclear regions allowing one to compare the capabilities of various theoretical models. For example, an extended study of non-yrast energy sequences with different parities has been implemented within the Extended Coherent States Model [13] by considering a coupling of the $\beta$ and $\gamma$ bands with respective bands possessing the same spins but opposite parities, as well as a coupling between $K^\pi = 1^+$ and $K^\pi = 1^-$ energy sequences. In the model scheme of the present work the positive-parity $\beta$-band appears connected to a negative-parity non-yrast sequence with odd angular momenta in the same way as in the yrast alternating-parity configuration. This is a consequence of the assumed mechanism of coupling between the quadrupole and octupole vibration modes. In this meaning the present consideration suggests a different band-coupling scheme and supposes a persistent role of the quadrupole-octupole motion in the forming of the higher-energy (non-yrast) part of the spectrum.

The paper is organized as follows. In Section 2 the CQOM model is presented and the model mechanism for the appearance of non-yrast alternating parity bands is shown. Numerical results and discussion on the application of the model in the regions of rare-earth nuclei and actinides are given in Section 3. Section 4 contains concluding remarks.

## 2 Model of Coherent Quadrupole–Octupole Motion

In the CQOM model [10] it is considered that the even–even nucleus can oscillate with respect to the quadrupole ($\beta_2$) and octupole ($\beta_3$) axial deformation variables, which are mixed through a centrifugal (rotation-vibration) interaction. The collective Hamiltonian of the nucleus is then taken in the form

$$H_{qo} \quad = \quad -\frac{\hbar^2}{2B_2}\frac{\partial^2}{\partial\beta_2^2} - \frac{\hbar^2}{2B_3}\frac{\partial^2}{\partial\beta_3^2} + U(\beta_2, \beta_3, I)\ , \tag{1}$$

where

$$U(\beta_2, \beta_3, I) = \frac{1}{2}C_2{\beta_2}^2 + \frac{1}{2}C_3{\beta_3}^2 + \frac{X(I)}{d_2\beta_2^2 + d_3\beta_3^2}\ , \tag{2}$$

with $X(I) = [d_0 + I(I+1)]/2$. $B_2$ and $B_3$ are effective quadrupole and octupole mass parameters and $C_2$ and $C_3$ are stiffness parameters for the respective oscillation modes. The quantity $\mathcal{L}^{(\text{quad+oct})} = (d_2\beta_2^2 + d_3\beta_3^2)$ can be associated to the moment of inertia of an axially symmetric quadrupole-octupole deformed shape with $d_2$ and $d_3$ being inertia parameters. The energy potential (2) represents a two-dimensional surface determined by the variables $\beta_2$ and $\beta_3$ with an angular-momentum-dependent repulsive core at zero deformation (see Figure 1 in [10]). The parameter $d_0$ in the centrifugal factor $X(I)$ characterizes the potential shape in the ground state and determines the overall energy scale for the rotation part of the energy.

If a condition for the simultaneous presence of nonzero coordinates $(\beta_2^{\text{min}}, \beta_3^{\text{min}})$ of the potential minimum is imposed, the stiffness and inertial parameters are correlated as $d_2/C_2 = d_3/C_3$ [10]. In this case the potential bottom represents an ellipse in the space of $\beta_2$ and $\beta_3$ which surrounds the infinite zero-deformation core (see Figure 3 in [10]). If prolate quadrupole deformations $\beta_2 > 0$ are considered, the system is characterized by oscillations between positive and negative $\beta_3$-values along the ellipse surrounding the potential core. By introducing polar variables

$$\eta = \sqrt{\frac{2(d_2\beta_2^2 + d_3\beta_3^2)}{d_2 + d_3}} \qquad \text{and} \qquad \phi = \arctan\left(\frac{\beta_3}{\beta_2}\sqrt{\frac{d_3}{d_2}}\right)\ ,$$

the potential (2) appears in the form

$$U_I(\eta) = \frac{1}{2}C\eta^2 + \frac{X(I)}{d\eta^2}\ , \tag{3}$$

where $C = (d/d_2)C_2 = (d/d_3)C_3$, with $d = (d_2+d_3)/2$. Further, by assuming that the quadrupole and octupole modes are represented in the collective motion with the same oscillation frequencies $\omega^2 = C_2/B_2 = C_3/B_3 \equiv C/B$, corresponding to a coherent quadrupole-octupole motion of the system, one obtains the model Hamiltonian in a simple form

$$H_{qo} = -\frac{\hbar^2}{2B}\left[\frac{\partial^2}{\partial\eta^2}+\frac{1}{\eta}\frac{\partial}{\partial\eta}+\frac{1}{\eta^2}\frac{\partial^2}{\partial\phi^2}\right]+U_I(\eta)\ . \tag{4}$$

It allows an exact separation of variables in the wave function $\Phi(\eta,\phi)=\psi(\eta)\varphi(\phi)$ with the subsequent equations for $\psi(\eta)$ and $\varphi(\phi)$

$$\frac{\partial^2}{\partial\eta^2}\psi(\eta)+\frac{1}{\eta}\frac{\partial}{\partial\eta}\psi(\eta)+\frac{2B}{\hbar^2}\left[E-\frac{\hbar^2}{2B}\frac{k^2}{\eta^2}-U_I(\eta)\right]\psi(\eta) = 0\ ; \tag{5}$$

$$\frac{\partial^2}{\partial\phi^2}\varphi(\phi)+k^2\varphi(\phi) = 0\ , \tag{6}$$

where $k$ is the separation quantum number. Equation (5) with the potential (3) has the following analytic solution for the energy spectrum [10]

$$E_{n,k}(I)=\hbar\omega\left[2n+1+\sqrt{k^2+bX(I)}\right], \tag{7}$$

where $\omega=\sqrt{C/B}$, $n=0,1,2,...$ and $b=2B/(\hbar^2 d)$. The respective eigenfunctions $\psi(\eta)$ are obtained in terms of the generalized Laguerre polynomials

$$\psi_n^I(\eta)=\sqrt{\frac{2\Gamma(n+1)}{\Gamma(n+2s+1)}}e^{-c\eta^2/2}(c\eta^2)^s L_n^{2s}(c\eta^2)\ , \tag{8}$$

with $c=\sqrt{BC}/\hbar$ and $s=(1/2)\sqrt{k^2+bX(I)}$. Equation (6) in the variable $\phi$ is solved under the boundary condition $\varphi(-\pi/2)=\varphi(\pi/2)=0$, which provides two different solutions with positive and negative parities, $\pi=(+)$ and $\pi=(-)$, respectively

$$\varphi^+(\phi) = \sqrt{2/\pi}\cos(k\phi)\ , \qquad k=1,3,5,...\ ; \tag{9}$$

$$\varphi^-(\phi) = \sqrt{2/\pi}\sin(k\phi)\ , \qquad k=2,4,6,...\ . \tag{10}$$

Since the consideration is restricted to axial deformations only, the projection $K$ of the collective angular momentum on the principal symmetry axis is taken zero. Then the total wave function of the coherent quadrupole-octuple vibration and collective rotation of an even-even nucleus has the form

$$\Psi^\pi_{nIM0}(\eta,\phi)=\sqrt{\frac{2I+1}{8\pi^2}}D^I_{M\,0}(\theta)\psi_n^I(\eta)\varphi^\pm(\phi)\ , \tag{11}$$

with the condition $\pi(-1)^I=1$ imposing positive parity for the states with even angular momentum, and negative parity for the odd angular momentum states.

The structure of the energy spectrum is determined by the quantum numbers $n$ and $k$ in (7). Here $n$ has the meaning of a "radial" phonon number, while $k$ corresponds to the number of "angular" phonons. Since according to (9) and (10)

$k$ obtains different values for the states with opposite parity the energy sequences with even and odd angular momenta corresponding to a given $n$ appear shifted to each other, i.e. a parity shift effect is observed. In [10] it was supposed that the GSB and the lowest negative-parity band belong to a $n = 0$ set with $k = k^{(+)} = 1$ for the GSB and $k = k^{(-)} = 2$ for the negative-parity band. In the present work the model scheme is extended through the following three suppositions.

i) The energy spectrum determined by the coherent axial quadrupole-octupole vibrations and rotations consists of couples of level-sequences with opposite parity. The sequences in each couple are characterized by the same value of the quantum number $n = 0, 1, 2, ...$ and by different values of $k$, $k = k_n^{(+)} = 1$ or $3$ or $5$ or ... for the even-$I$ sequence, and $k = k_n^{(-)} = 2$ or $4$ or $6$ or ... for the odd-$I$ sequence.

ii) The lowest values of the "radial" quantum number $n$ correspond to the lowest alternating parity bands, with $n = 0$ being the yrast band, $n = 1$ corresponding to the next non-yrast alternating parity structure and so on. The values of the "angular" quantum number $k$ are not restricted and should only satisfy the parity condition in i). The particular values of $k_n^{(+)}$ and $k_n^{(-)}$ can be determined so as to reproduce the experimentally observed parity shift in the set of levels with a given $n$.

iii) Due to the coherent interplay between the $\beta_2$ and $\beta_3$ variables in the oscillation motion, the excited $\beta$- bands in even-even nuclei can be interpreted as the positive-parity counterparts of higher negative parity sequences, or as the members of non-yrast alternating parity bands.

Based on the above assumptions the extended alternating-parity spectrum of a even-even nucleus can be considered in the following form.

Yrast alternating-parity set ($n = 0$): unites the GSB ($k = k_0^{(+)}$) $I_\nu^\pi = 2_1^+, 4_1^+, 6_1^+$, ..., with the first negative-parity band ($k = k_0^{(-)}$) $I_\nu^\pi = 1_1^-, 3_1^-, 5_1^-$, ...;

First non-yrast set ($n = 1$): unites the first $\beta$-band ($k = k_1^{(+)}$) $I_\nu^\pi = 0_1^+, 2_2^+, 4_2^+$, ..., with the second negative-parity band ($k = k_1^{(-)}$) $I_\nu^\pi = 1_2^-, 3_2^-, 5_2^-$, ...;

Second non-yrast set ($n = 2$): unites the second $\beta$-band ($k = k_2^{(+)}$) $I_\nu^\pi = 0_2^+, 2_3^+, 4_3^+$, ... with the third negative-parity band ($k = k_2^{(-)}$) $I_\nu^\pi = 1_3^-, 3_3^-, 5_3^-$, ..., and so on, higher non-yrast sequences, where $\nu = 1, 2, 3, ...$ is the consequent number of the appearance of an excitation with a given angular momentum.

Obviously the above model scheme makes no claim to exhaust the entire collective spectrum but rather provides a tool to identify the extent to which the considered quadrupole-octupole motion can influence the excited band structures in even-even nuclei. In the end of this section, it should be remarked that the extension of the model to higher energy levels, together with assumption ii), which releases $k$ from the fixed values $k^{(+)} = 1$ and $k^{(-)} = 2$ (originally imposed in [10] for the yrast case), now requires a new readjustment of the model parameters.

## 3 Numerical results and discussion

The CQOM model scheme is applied to several rare-earth and actinide nuclei. The model parameters $\omega$, $b$ and $d_0$, entering the theoretical energy $\tilde{E}_{n,k}(I) = E_{n,k}(I) - E_{0,0}(0)$, are adjusted to the experimental data with the values of the quantum numbers $k_n^{(\pm)}$ being chosen to provide best agreement between theory and experiment. The theoretical and experimental levels of the considered nuclei are compared in Figures 1-6. All experimental data are taken from [14]. In Figure 1 the results for the nuclei $^{152}$Sm, $^{154}$Sm, $^{150}$Nd and $^{156}$Dy are shown. A good quality of the model description is observed with the root mean-square (RMS) deviation between the theory and experiment being in the limits of 30–60 keV. Some higher energy negative parity levels in the yrast sequences of $^{150}$Nd and $^{154}$Sm as well as a $1^-$ level in the first non-yrast sequence in $^{156}$Dy not available in the data base [14] are predicted. For the nuclei $^{150}$Nd, $^{152}$Sm and $^{156}$Dy whose yrast alternating parity sequences were described in [10] now descriptions of the first non-yrast sequences are already available. One should remark that the extended model descriptions are characterized by new sets of model parameters, as well as by new couples of values of the quantum numbers $(k_0^{(+)}, k_0^{(-)})$ for the yrast sequences. For example in $^{152}$Sm presently one has

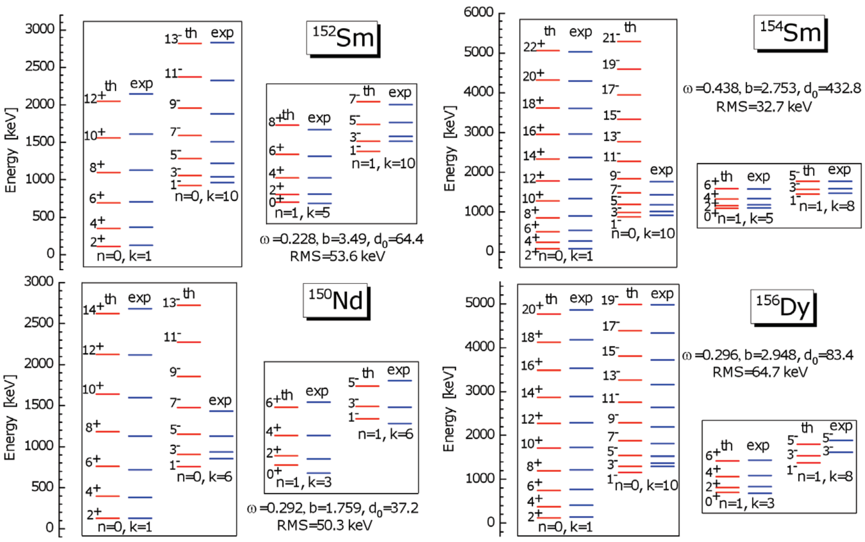


Figure 1. Theoretical and experimental alternating parity spectra for $^{152}$Sm, $^{154}$Sm, $^{150}$Nd and $^{156}$Dy. The values of the quantum numbers $n$ and $k$ used in the model description are given below the respective level-sequence. The values of $\omega$ are given in MeV/$\hbar$, while $b$ and $d_0$ are in units $\hbar^{-2}$ and $\hbar^2$, respectively. The root mean-square (RMS) deviation between theory and experiment is also given.

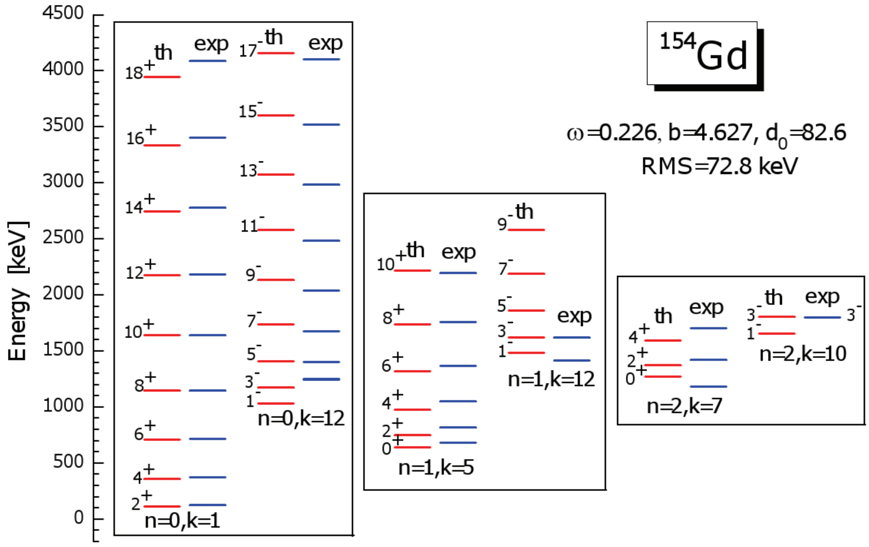


Figure 2. Same as in Figure 1, but for $^{154}$Gd.

$k_0^{(+)} = 1$ and $k_0^{(-)} = 10$, while in [10] these values are $k_0^{(+)} = 1$ and $k_0^{(-)} = 2$.

In Figure 2 the result for the nucleus $^{154}$Gd is shown. Here in addition to the yrast band and the first excited band, a second excited sequence is also

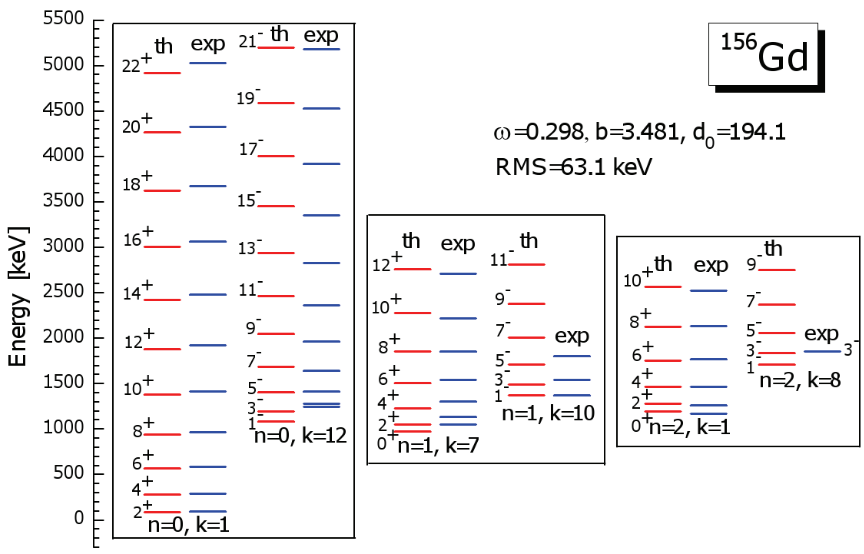


Figure 3. Same as in Figure 1, but for $^{156}$Gd.

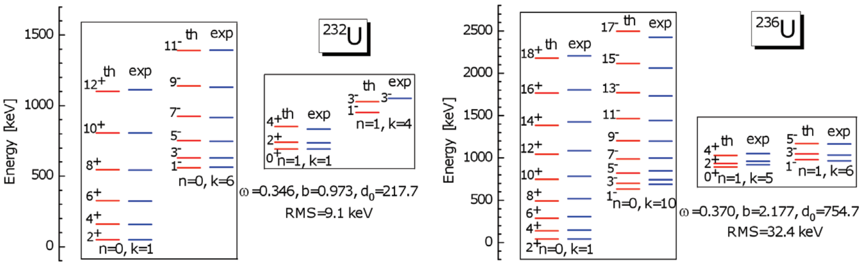


Figure 4. Same as in Figure 1, but for $^{232}$U and $^{236}$U.

described. Although it is not well experimentally developed, three levels of the second $\beta$ band and a third excited $3^-$ level are described, while a third excited $1^-$ level is predicted. One should remark that the belonging of the considered $3^-$ state to given collective structure of the spectrum is not well established in the experiment. Although the data show that it can be included into a negative parity sequence containing odd and even angular momentum values $(2^-, 3^-, 4^-, ...)$ the present description suggests that it could be also classified as a part of an excited alternating parity sequence. As in the case of Nd and Sm nuclei, the non-yrast levels in $^{154}$Gd are described in addition to the previously considered [10] yrast band. Again, one observes a readjustment of the model parameters and a change in the values of the quantum number $k$, $(k_0^{(+)} = 1, k_0^{(-)} = 12)$, for the

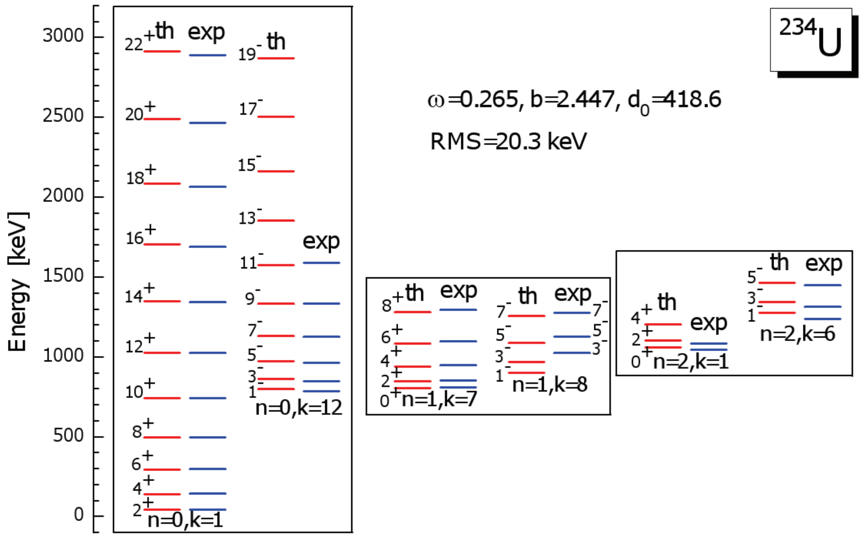


Figure 5. Same as in Figure 1, but for $^{234}$U.

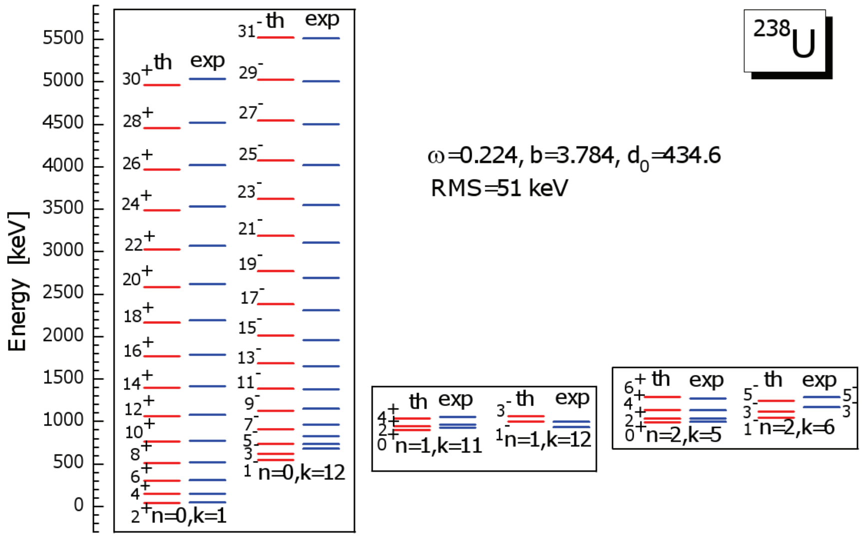


Figure 6. Same as in Figure 1, but for $^{238}$U.

yrast band. In Figure 3 similar result with a bit better developed yrast and beta bands is shown for the nucleus $^{156}$Gd.

In Figure 4 results from the first-time application of CQOM in the actinide region are shown for the nuclei $^{232}$U and $^{236}$U. One sees that the experimentally observed yrast and first excited level sequences are quite well described. In Figures 5 and 6 the long yrast alternating parity sequences in $^{234}$U and $^{238}$U are described together with the first and second excited non-yrast sequences. Similarly to $^{154}$Gd and $^{156}$Gd the belongings of the second negative-parity level-sequence in $^{234}$U and the third negative-parity sequence in $^{238}$U are not clear. Therefore, the present model description can be considered as a theoretical suggestion for a possible collective classification of these levels.

## 4 Conclusion

The present work provides a description and respective classification of yrast and non-yrast alternating parity sequences in rare-earth and actinide nuclei within the collective model of coherent quadrupole and octupole motion (CQOM). The model formalism and the quality of the obtained descriptions show the possible developing of nuclear alternating parity spectra towards quite high non-yrast regions of excitation. The obtained results suggest that in the regions with reflection asymmetric degrees of freedom the quadrupole-octupole motion of the system determines not only the low-lying energy levels, but also the higher-energy collective properties of nuclei. More detailed conclusions about the evolution of the alternating parity spectra in the different nuclear regions can be obtained by extending the range of the model description to other nuclei as well as by examining the electric transition probabilities, especially E1 and E3, in these spectra. Work in this direction is in progress.

## Acknowledgements

This work is supported by DFG and by the Bulgarian National Science Fund (contract DID-02/16-17.12.2009).

## References

[1] P.A. Butler and W. Nazarewicz, *Rev. Mod. Phys.* **68** (1996) 349.
[2] H.J. Krappe and U. Wille, *Nucl. Phys. A* **124** (1969) 641.
[3] G.A. Leander, R.K. Sheline, P. Möller, P. Olanders, I. Ragnarsson, and A.J. Sierk, *Nucl. Phys. A* **388** (1982) 452.
[4] R. Jolos, P. von Brentano, and F. Dönau, *J. Phys. G: Nucl. Part. Phys.* **19** (1993) L151.
[5] V.Yu. Denisov and A.Ya. Dzyublik, *Nucl. Phys. A* **589** (1995) 17.
[6] N.V. Zamfir and D. Kusnezov, *Phys. Rev. C* **63** (2001) 054306.
[7] T.M. Shneidman, G.G. Adamian, N.V. Antonenko, R.V. Jolos and W. Scheid, *Phys. Lett. B* **526** (2002) 322; *Phys. Rev. C* **67** (2003) 014313.
[8] A.A. Raduta, D. Ionescu, I.I. Ursu and A. Faessler, *Nucl. Phys. A* **720** (2003) 43.
[9] N. Minkov, P. Yotov, S. Drenska and W. Scheid, *J. Phys. G: Nucl. Part. Phys.* **32** (2006) 497.
[10] N. Minkov, P. Yotov, S. Drenska, W. Scheid, D. Bonatsos, D. Lenis and D. Petrellis, *Phys. Rev. C* **73** (2006) 044315.
[11] P.G. Bizzeti and A.M. Bizzeti-Sona, *Phys. Rev. C* **77** (2008) 024320.
[12] B. Buck, A.C. Merchant and S.M. Perez, *J. Phys. G: Nucl. Part. Phys.* **35** (2008) 085101.
[13] A.A. Raduta, Al.H. Raduta, and C.M. Raduta, *Phys. Rev. C* **74** (2006) 044312.
[14] http://www.nndc.bnl.gov/ensdf/.